



## Utilization of the time-temperature gradient post annealing process for enhancing femtosecond laser induced damage threshold of $\text{TiO}_2$ optical films/ verification by XPS study

Alireza Bananej<sup>\*1</sup>, Mahdieh Khatiri<sup>1</sup>, Hossein Shahrokhabadi<sup>1</sup>, Zohreh Parsa<sup>2</sup>, Hadi Adelkhani<sup>3</sup>

<sup>1</sup>Photonics and quantum technology research school, Nuclear Science and Technology Research Institute

<sup>2</sup>Kharazmi university, Physics Department, Iran

<sup>3</sup>Nuclear fuel cycle research school, Nuclear Science and Technology Research Institute

E-mail: arbananej@yahoo.com, abananeg@aeoi.org.ir

(Received 29 December 2024; in final form 06 May 2025)

### Abstract

In this study we have investigated the effect of controlled post annealing process on the optical properties, chemical composition, and theoretical predictions of femtosecond laser induced damage threshold of  $\text{TiO}_2$  thin films. It has been shown, by using time temperature gradient annealing process, optical properties of the deposited films can be tailored, and hence, predicted ultra-fast laser induced damage threshold can be enhanced considerably. Also, the above results were in a good agreement with the XPS results of the deposited samples at two distinct annealing processes.

**Keywords:** Damage threshold, Femtosecond laser, Annealing, Time- temperature gradient, Xray photoelectron spectroscopy

### 1. Introduction

Power of laser systems can be increased dramatically by using different techniques such as chirped pulse amplification [1]. But, the main bottleneck for scaling up the power of laser systems practically, is the damage threshold of optical materials, especially, optical coatings [2]; so research about fabrication of thin films with higher laser induced damage threshold (LIDT) is one of the most important subjects in the high power lasers studies.

Ultra-short pulse laser induced damage mechanism is quite different than nanosecond regime [3]. In nanosecond regime the LIDT mechanism in optical coatings is a statistic phenomenon which is due to absorption of laser energy on the defect points which are randomly distributed along the thin film surface. Therefore, the main approach for improving the LIDT in long pulse regime of laser radiation is focused on the enhancement of thermal properties of the optical coatings such as thermal conductivity. it has been shown that films with high thermal conductivity have higher LIDT parameter [4].

But, in femtosecond regime of pulse duration, the laser damage is mainly governed by the ablation process which is dominated by the intrinsic properties of the materials such as band gap energy ( $E_g$ ) and refractive index ( $n$ ) of the materials. In femtosecond pulse range, photoionization and electron impact ionization are the two main mechanisms that they can produce high electron

density in the conduction band which caused laser damage [5, 6].

Recently there has been tremendous effort on the experimental and theoretical analysis for estimating the LIDT of optical coatings in ultra-short pulse regime of laser radiation, Mero et al., [5] derived an experimental linear relationship between Ultra-fast LIDT and dielectric thin film band gap energy, and Mangote et al; [7] derived an empirical inverse cubic monomial correlation between femtosecond LIDTs and refractive index of oxide thin films. Deviation from the both mentioned approaches are evidenced by Mangote et al; [7]. The theoretical model presented by Shahrokhabadi et al; [8] results in more accurate reproduction of experimental data of ultra-fast LIDT. In this sense, we proposed the improvement of femtosecond LIDT in main optical coatings such as  $\text{TiO}_2$  by the manipulation of refractive index and band-gap energy.

Recently it has been shown that time temperature gradient annealing (TTGA) process can be improved LIDT at long pulse regime of pulse radiation for  $\text{ZrO}_2$  as one of the main optical thin films for hard coatings. In this study it has been shown that by using TTGA, the damage threshold of  $\text{ZrO}_2$  can be enhanced to  $14.88 \text{ J/cm}^2$  in long pulse, nanosecond, regime of radiation [9].

In this paper we try to investigate the effect of TTGA on LIDT at short pulse regime of pulse radiation.

**Table 1.** conditions of depositions process.

Base pressure of the vacuum chamber (torr)	$10^{-5}$
Partial pressure of Oxygen (torr)	$6 \times 10^{-5}$
Deposition rate (nm/s)	0.1
Deposition temperature (°C)	200
thin films Thickness (nm)	200

**Table 2.** Details of heat treatment process

Sample ID	Heat treatment process	Time-Temperature gradient
$S_{\text{Rate}}$	Temperature of the oven was increased $2.2^{\circ}\text{C}$ for each minute up to $400^{\circ}\text{C}$ .	Rate
$S_{\text{step}}$	Temperature of oven was set for one-hour respectively $200^{\circ}\text{C}$ , $300^{\circ}\text{C}$ and $400^{\circ}\text{C}$ .	Step
$S_{\text{fix}}$	The oven worked in the fix temperature $400^{\circ}\text{C}$ for 3 hours.	Very fast (ordinary annealing process)

Therefore, after preparation of  $\text{TiO}_2$  films on Bk7 substrates, they had exposed under special annealing treatment rather than ordinary annealing process. Next, we calculated band-gap energy and refractive index for all samples and finally calculate ultra-fast LIDT in the range of femtosecond pulse duration. The results show, as a consequence of using special TTGA process, the femtosecond LIDT can be improved considerably, which is agree with XPS study.

## 2. Experiments

### 2.1 $\text{TiO}_2$ thin film preparation

Electron beam evaporation method was applied to deposit 200nm of  $\text{TiO}_2$  thin films on the Bk7 substrates. Deposition conditions are presented in Table 1. After deposition process, thin films were heated in an oven with three different time-temperature gradients in atmospheric pressure. The details of the heating methods are given in Table 2.

### 2.2- UV-Visible spectrum and refractive index measurement

Transmission curves of all samples were measured with a dual beam spectrophotometer device with accuracy of 0.03%. In this device the initial optical beam is split into two beams; one of which is directly transmitted to the detector, and the other one is transmitted through the sample and is compared with the reference beam. Based on the measured spectra which are illustrated in figure 1 decreasing in heating rate results in increase of samples' transmittance in the visible range. Refractive indices of the deposited samples are calculated by using envelop method [10]. Figure 2, shows refractive indices of samples versus wavelength. As a reason of figure 2 refractive index of deposited thin films, decrease by the reduction of heating rate. Also calculated refractive index converges to a non-dispersive value as expected.

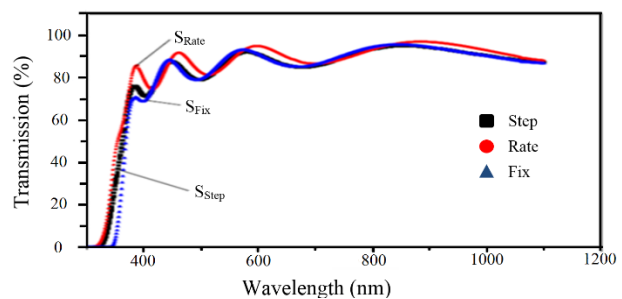


**Figure 1.** Measured transmission spectra of the deposited  $\text{TiO}_2$  samples at different TTGA process.

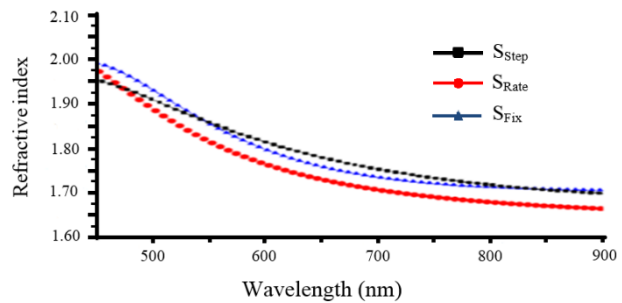


**Figure 2.** Calculated refractive index of the deposited  $\text{TiO}_2$  thin films at different TTGA process.

### 2.3- Optical band gap of $\text{TiO}_2$ thin films and femtosecond LIDT measurement

The optical bandgap of  $\text{TiO}_2$  films can be determined by using Tauc [11] relation. According to this relation the absorption coefficient has the following energy dependence

$$\alpha = \frac{B_1(hv - E_g)^{1/r}}{hv} \quad (1)$$

Where  $B_1$  is constant, and  $r=1/2, 2, 3/2$  or  $3$  for allowed direct, allowed indirect, forbidden direct and indirect electronic transition, respectively. So, the whole band gap of  $\text{TiO}_2$  film can be determined by plotting  $(\alpha h\nu)^2$  versus  $(h\nu)$  and extrapolating the linear region of the plot toward low energy ( intersection of tangential with horizontal axis). This method is an approximation for allowed direct electronic band to band transition in semiconductors, because it assumed that the refractive index is constant in the considered energy range.

On the other hand, absorption coefficient of thin films can be calculated by using envelope methods and having transmittance and refractive index curves by using following relation [10]

$$\alpha = -\frac{1}{t} \ln \frac{(n-1)(n-n_s)(\frac{T_{\min}}{T_{\max}}+1)^{0.5}}{(n+1)(n+n_s)(\frac{T_{\max}}{T_{\min}}-1)^{0.5}} \quad (2)$$

In Eq. (2)  $T_{\max}$  and  $T_{\min}$  are maximum and minimum transmission in a specific wavelength.  $n$  and  $n_s$  are refractive indices of thin film and substrate, respectively and  $t$  is thin film thickness and equals to 200nm. By using Eq. (1) and Eq. (2) we can plot  $(\alpha h\nu)^2$  as function of  $h\nu$ , as shown in figure 3. according to Tauc model, we can find the bandgap energy [11].

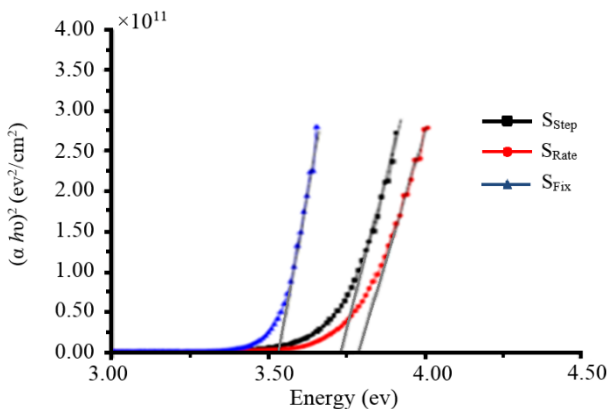


**Figure 3.** Variation of  $(\alpha h\nu)^2$  as function of photon energy ( $v\nu$ )

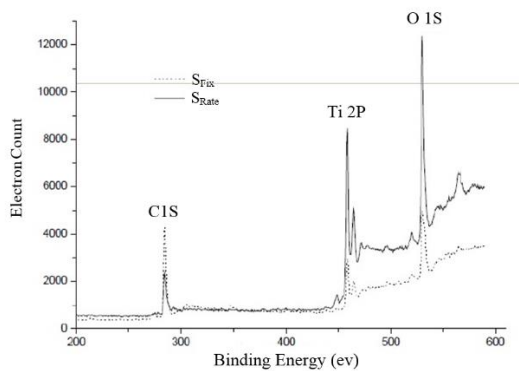


**Figure 4.** Wide range XPS spectrum of the prepared  $\text{TiO}_2$  layers. Three large peaks indicate the presence of Oxygen (O 1S), Titanium (Ti 2P) and Carbon (C 1S) in the thin films.

Ultra-fast laser induced damage threshold of wide band-gap optical thin films such as  $\text{TiO}_2$  can be determined by using the following expression [8]

$$\text{LIDT} = \frac{A}{(n^2-1)E_g} \quad (3)$$

In Eq. (3) A is the fitting constant which depends on the pulse length as well as temporal duration. n and  $E_g$  are standing for refractive index and band-gap energy respectively.

#### 2.4- XPS analysis

In this section, according to figure 3, which shows a distinct change of band gap energy for  $S_{\text{rate}}$  and  $S_{\text{fix}}$ , we study the XPS spectra just for these two samples as below: Concentric hemispherical energy analyzer is utilized to perform XPS study of the prepared thin films. Atomic combination, as well as, stoichiometry of the deposited layers are deduced from the measured XPS spectrum. In the case of  $S_{\text{Step}}$ , refractive index and band gap energy lie between  $S_{\text{Fix}}$  and  $S_{\text{Rate}}$  samples. So, we excluded this sample from the XPS analysis. Figure 4 illustrates the measured XPS spectrum of the deposited thin films in the binding energy range of 0.2 to 0.6 Kev. Existence of Ti, O and C (because of contamination) on the surface of samples is evident in figure 4. Also, figure 5. shows higher resolution of XPS spectrum. In this spectrum the doublet  $\text{Ti}_{2\text{P}}^{3/2}$  (binding energy 458.6 eV) and  $\text{Ti}_{2\text{P}}^{1/2}$  (binding energy 464.4 eV) arises from Spin orbit coupling that leaded to the 2P splitting to the  $\text{Ti}_{2\text{P}}^{1/2}$  and  $\text{Ti}_{2\text{P}}^{3/2}$ . These peaks are consistent with  $\text{Ti}^{4+}$  in  $\text{TiO}_2$  lattice [12,13].

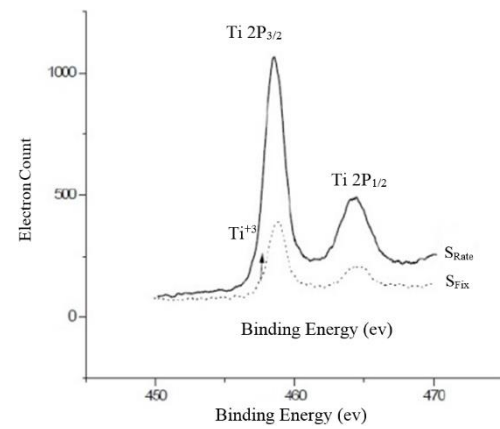


**Figure 5.** Precise XPS scan of the deposited  $\text{TiO}_2$  layers in the energy range

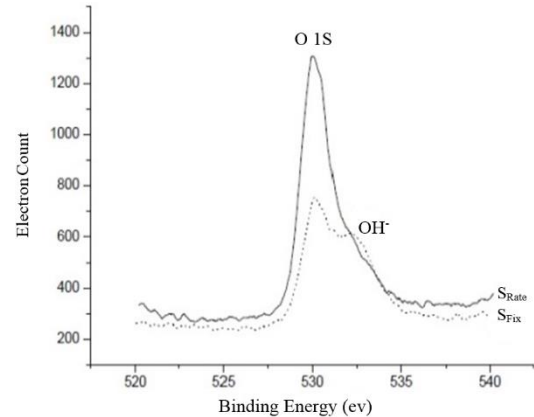


**Figure 6.** Precise XPS scan of the deposited  $\text{TiO}_2$  layers in the energy range associated to the Oxygen anions (O1s) and Hydroxyl anions (OH<sup>-</sup>).

Absence of electron count peak in the near vicinity of 458 eV in both XPS spectrums indicates the omission of  $\text{Ti}^{4+}$  in  $\text{Ti}_2\text{O}_3$  chemical formula. This is due to the positive impact of the annealing process. The area of  $\text{Ti}_{2\text{P}}^{3/2}$  and  $\text{Ti}_{2\text{P}}^{1/2}$  peaks in figure 5 represent the amount of  $\text{Ti}^{4+}$  and hence  $\text{TiO}_2$  in the deposited thin films. Figure 5 demonstrates that in the case of  $S_{\text{rate}}$   $\text{TiO}_2$  compound is more dominant than the other annealing approach.

By zooming in the energy interval from 520 to 540 eV, we can estimate the relative presence of oxide anion ( $\text{O}^{2-}$ ) and hydroxyl compound. The area of O<sub>1s</sub> peak shows the amount of oxide anion and the area under the OH<sup>-</sup> represents the ratio of hydroxyl compounds due to the defects and contaminations [13]. Figure 6 illustrates that, the amount of oxide anions which is associated with  $\text{TiO}_2$  dramatically increased in the case of  $S_{\text{rate}}$ . In addition, the surface below the OH<sup>-</sup> vanished to zero when the appropriate annealing process of  $S_{\text{rate}}$  is employed according to the figure 6.

### 3. Results and discussion

As a result of figure 2 and figure 3 It can be seen that different TTGA process leads to changing of optical band gap energy, and refractive index of the deposited thin films which is shown in Table 3.

**Table 3.** Optical properties, grain size [14], and normalized ultra-fast LIDT of the deposited samples.

Sample	Optical band gap (ev)	Refractive index	Grain size [14] (nm)	Normalized ultra-fast LIDT
$S_{\text{Rate}}$	3.78	1.66	28.57	1
$S_{\text{step}}$	3.73	1.70	27.86	0.93
$S_{\text{fix}}$	3.53	1.72	27.76	0.95

According to Table 3, by using rate TTGA process, (as  $2.2^{\circ}\text{C}/\text{min}$  up to  $400^{\circ}\text{C}$ ), the optical band gap increased in comparison to two other TTGA process. In addition, reduction of the refractive index of the synthesized thin films by the application of the rate TTGA process is illustrated in Table 3. Also, it has been shown the sample which has the slower heating rate grows with good crystal lattice and it has larger grain size [13]. Direct relationship between grain size and short pulse LIDT is explained by Yang et. al. [15]. Presented results in the two last columns of the Table 3 confirms the experimental investigations in this case. According to the published scientific report, dielectric materials with lower values of  $(n^2 - 1)E_g$  exhibit higher ultra-fast LIDT [8]. Therefore, normalized ultra-fast LIDT of the deposited thin films can estimated by the Eq. (3). Elevation of femtosecond LIDT by the reduction of the temperature rate (in the case of  $S_{\text{rate}}$ ) in the heat treatment process is demonstrated in the Table 3. Also, as a reason of figure 5, higher area of the peak of  $2p_{1/2}$  and  $2p_{3/2}$  of  $S_{\text{rate}}$ , shows better stoichiometric of  $\text{TiO}_2$  with respect to  $S_{\text{fix}}$  which results improvement of ultra-fast LIDT by using TTGA process.

On the other hand, annihilation of the XPS peak associated to the hydroxyl compounds as shown in figure 6, Shows the positive impact of TTGA process. It is apparent that the optical bandgap increases with increaseing grain size.

This fact is in a good agreement with the known effect as “Burstein-Moss effect” that state larger grain size leads to fewer defects and finally, rising numbers of free electrons in the conduction band so with increasing free charge carriers, the optical band gap increases, which can be attributed to quantum confinement. Finally, as a reason of Eq.3, increasing the optical band gap leads to increasing of LIDT at short pulse laser radiation [16].

## 5. Conclusion

In conclusion, 200 nm of  $\text{TiO}_2$  films were deposited on Bk7 optical glass by using electron beam evaporation method.

As a reason of positive impact of TTGA process for long pulse regime, we investigate this method for femto - second regime of radiation. For this purpose the deposited samples were annealed through the TTGA process. transmission spectrum of samples were measured and by using envelope method refractive index and absorption coefficient were measured. Also, the bandgap energy were calculated. According to the theoretical relation for femto second LIDT, it can be seen that the calculated LIDT for sample with slowly TTGA process (  $S_{\text{rate}}$  ) enhanced considerably. This fact is in a good agreement with XPS study which state, the amount of  $\text{TiO}_2$  in slowly varying annealing process sample,(  $S_{\text{rate}}$  ), is much higher than other sample where leads to enhancement of the femto second LIDT.

## References

1. P Maine, et al, IEEE Journal of Quantum electronics **24**(2) (1988) 398.
2. D Ristau, CRC Press (2014).
3. A C Tien, et al, , Physical Review Letters **82**(19) (1999) 3883.
4. A Bananej, et al, Optics & Laser Technology **42**(8) (2010)1187.
5. M Mero, et al , Physical Review B **71** (11) (2005) 115109.
6. H Shahrokhabadi, et al, Thin Solid Films **669** (2019)168.
7. M Magnote, et al, Optics letters **37** (9) (2012) 1478.
8. H Shahrokhabadi, et al , Thin Solid Films **636** (2017) 289.
9. A Hassanpour, et al , Applied Surface Science (2012) 2395.
10. M Calgar,et al, Journal of Optoelectronics and Advanced Materials **8** (4) (2006)1410.
11. Tauc, J. Materials Research Bulletin. **3** (1968) 37. doi:10.1016/0025-5408(68)90023-8.
12. B Bharti, et al, Scientific Reports **6** (1) (2016)1.
13. P Babelon, et al, Thin Solid Films **322**(1-2) (1998)63.
14. A Hassanpour, et al, Optik **124** (1) (2013) 35.
15. C Yang, et al, Applied Surface Science **254** (9) (2008) 2685.
16. Burstein, Elias , Physical Review (1954) 632.